CREEP DEFORMATION OF B2 ALUMINIDES

M. V. Nathal
NASA Lewis Research Center
Cleveland, OH USA 44135

ABSTRACT. The creep resistance and elevated temperature deformation mechanisms in CoAl, FeAl, and NiAl are reviewed. The stress and temperature dependencies of the steady state creep rate, the primary creep behavior, the dislocation substructure, and the response during transient tests are used as the main indicators of the deformation processes. In single phase intermetallics, the influence of grain size, stoichiometry, and solid solution hardening have been examined. In addition, the effect of adding dispersoids, precipitates, and other types of reinforcements to improve creep strength are compared.

1. INTRODUCTION

The B2 structure aluminides CoAl, FeAl, and NiAl have several attributes which provide a basis for interest as high temperature structural materials. They have low densities, relatively high melting points, and the potential for excellent oxidation resistance. In addition, their simple cubic crystal structures and large solubility ranges allow alloy design flexibility for improved properties over those of the binary compounds. Creep resistance is one of the important properties required for extended use at high temperatures. Of course, in most conditions a balance of high temperature creep strength, low temperature fracture toughness, and environmental resistance is required. This paper will not address the difficult challenge of achieving the required balance in properties; however, it should be kept in mind that in many cases improvements in one area result in a degradation in other properties.

The review is divided into two main parts. First, the creep behavior of the binary, single phase compounds is presented, and both diffusional and dislocation creep are discussed. The second part will describe the attempts at improving the creep strength of these intermetallics. The vast majority of these strategies involves adding a reinforcing second phase. It will become readily apparent that the amount of work performed on NiAl far exceeds that of both CoAl and FeAl combined. CoAl appears to be hampered by its low toughness values coupled with no advantages over NiAl in either density or melting point. FeAl, despite its higher levels of ductility, is limited to lower temperatures by its strength, melting point, and oxidation resistance.

2.0 CREEP OF BINARY COMPOUNDS

Creep deformation of the B2 aluminides follows that for metals and alloys and can be divided into primary, secondary and tertiary stages. The shape of the primary creep curve provides an important clue for determining the deformation mechanisms, although the secondary stage is usually of more interest because it tends to comprise the majority of

the creep life. The tertiary stage has rarely been examined in these materials, primarily because most testing to date has been in compression, where tertiary creep is suppressed or eliminated.

The second stage or steady-state creep rate ϵ is usually expressed as a form of the Dorn equation(1):

$$\epsilon = A\sigma^n \exp(-Q/RT) \qquad [1]$$

Here σ is the applied stress, n is the stress exponent, Q is the activation energy for creep, R is the gas constant, T is the absolute temperature, and A is a constant which includes microstructural variables such as grain size and stacking fault or anti-phase boundary energy. The values for the various parameters in Eqn. 1 are dependent on the operative deformation mechanisms within a given temperature and stress regime. Although the existence of a true steady state is difficult to substantiate, it is usually a satisfactory approximation; as an alternative, a minimum creep rate can usually be substituted with consistent results. Another important point implied by Eqn. 1 is that the steady-state creep rate is independent of test mode. Although creep tests have traditionally been performed under constant load or constant stress conditions, with the steady state strain rate measured as the dependent variable, it is equally valid to impose a constant strain rate and measure the steady state flow stress as the dependent variable. This has been experimentally verified for a number of systems(2,3) with known exceptions that can be traced to microstructural instabilities(4).

2.1 Dislocation Creep

Dislocation creep mechanisms are well described by the above semi-empirical equation, although the details of the mechanisms themselves are being continuously refined(5). For single phase metals and alloys, dislocation creep can be classified as either of two main types, known as Class M, or pure metal type, and Class A, or alloy type(5-7). Class M creep is characterized by glide being much faster than climb, and thus creep becomes controlled by the rate of climb past substructural obstacles. Class A creep is often called viscous glide controlled creep, since the glide of dislocations is restricted by solute atoms or perhaps by a high lattice friction stress due to long range order. This reduced glide mobility is the limiting creep process, while climb can occur readily. Although these categories represent limiting conditions, and many materials exhibit an intermediate behavior comprised of a mixture of the defining traits, these two types of behavior can be distinguished by several criteria(1,5-7), as listed in Table I. The most commonly used indicator for determining the deformation behavior is the stress exponent, which takes on values close to 5 for Class M and 3 for Class A. The activation energy for creep is equal to that for lattice diffusion regardless of the mechanism, although corrections for the temperature dependence of the elastic modulus are frequently necessary(1,8). In terms of dislocation structure, Class M materials tend to form subgrains during creep, while in Class A materials, a uniform distribution of dislocations is developed. The two types also have different primary creep behavior. For Class M materials in a constant load (or constant stress) test, a normal primary creep region is exhibited, in which the creep rate is initially high and decreases to the steady state value as the subgrains form. This is in contrast to an

inverted primary region seen in Class A materials, where the creep rate is initially low but increases to the steady value. If the test is performed under constant crosshead speed (or strain rate) conditions instead of constant load, the analogous behaviors of work hardening or yield points are observed(2). Finally, there are tests which are important for discriminating between mechanisms, whereby sudden changes in applied stress or strain rate are made and the responses are unique to the material and the type of test(5,9,10). For example, the instantaneous strain increment after a small stress increase would be primarily elastic for Class A materials but would have a large plastic component in Class M behavior.

TABLE I
Criteria For Classifying Dislocation Creep Behavior

	Class M	Class A
Controlling Mechanism	Climb	Viscous Glide
n	5	3
Q	Diffusion	Diffusion
Dislocation Structure	Subgrains	Homogeneous
Primary Creep const.σ const.$\dot{\epsilon}$	Normal Work Hardening	Inverted Yield Point
Response To Transients	Class M	Class A

A summary of the stress exponents and activation energies determined by various authors(11-23) is presented in Table II. For NiAl and CoAl, the best choice for activation energy appears to be close to 310 kJ/mol, which is reasonably close to the activation energies determined in diffusion experiments(24-28). For FeAl, however, an activation energy for creep of ~450 kJ/mol is much higher than that for diffusion, ~300 kJ/mol(28-30). Correction for the temperature dependence of the elastic modulus, using dynamic moduli(31,32) results in reductions in Q ranging from 15 Kj/mol in CoAl to 40 kJ/mol in FeAl, which is not sufficient to explain the discrepancies observed for FeAl. Certainly, the larger number of both diffusion and creep studies which have been conducted on NiAl allows for more confident analyses compared to either FeAl and CoAl.

Fig. 1 presents a summary of the creep data for NiAl at 1175 K, a temperature chosen because it required the least amount of interpolation. Most of the data from the various studies cluster with reasonable agreement, within about a factor of 5 in creep rate at a given stress level, and the stress exponents are also similar, between about 4.5 to 6. The early data by Vandervoort et al.(16) appears to be abnormally weak for no known reason. Fig. 2 shows the stress exponent as a function of temperature and compiles data generated from many studies on NiAl. Included in this plot are data from materials having a wide variety of grain sizes, including single crystals. Below about

TABLE II
Summary of Creep Parameters for B2 Aluminides

At% Al	Grain Size (μm)	T (K)	n	Q (kJ/mol)	Reference
NiAl					
48.25	5-9	1000-1400	6-7.5	313	11
49.2	15-20	1100-1400	5.75	314	12
50	12	1200-1300	6	350	13
50	450	1073-1318	10.2-4.6	283	14
50	500	1173	4.7	--	15
50.4	1000	1075-1750	7-3.3	230-290	16
50	SX[123]	1023-1223	7.7-5.4	--	17
50	SX	1023-1328	4-4.5	293	18
50	SX[001]	1000-1300	6	440	19
CoAl					
44	8	1100-1400	2.7	200	20
49.9	10	1100-1400	4.5	345	20
50	20	1200-1300	3	384	21
50	SX[123]	1323	2.6	--	17
FeAl					
27	70	810-1010	6	370	22
45.7	40	1300-1400	3.5	410	23
48.7	40	1100-1200	6.5	470	23
50	500	1173	4.0	--	15

1000-1100 K, the stress exponent starts to rise drastically, indicating a transition between high temperature creep and lower temperature behavior which can perhaps be called power-law breakdown. Discounting the abnormally weak material of Vandervoort et al., this figure reveals that between ~1100-1400 K, the values for n cluster between about 5 and 7. Although a stress exponent of 7 is higher than typical, such high values have been observed in several Class M materials(35,36). Combined with the stress exponent data, the other criteria listed in Table I have also been examined. Observations of subgrain formation after high temperature deformation have been made by numerous workers(11-15,37-40), and normal primary creep behavior, under both constant load and constant crosshead speed conditions, has also been observed(11-13,39,41). Additionally, the strain rate transient tests performed by Yaney and Nix(41) have also been consistent with Class M behavior. So in summary,

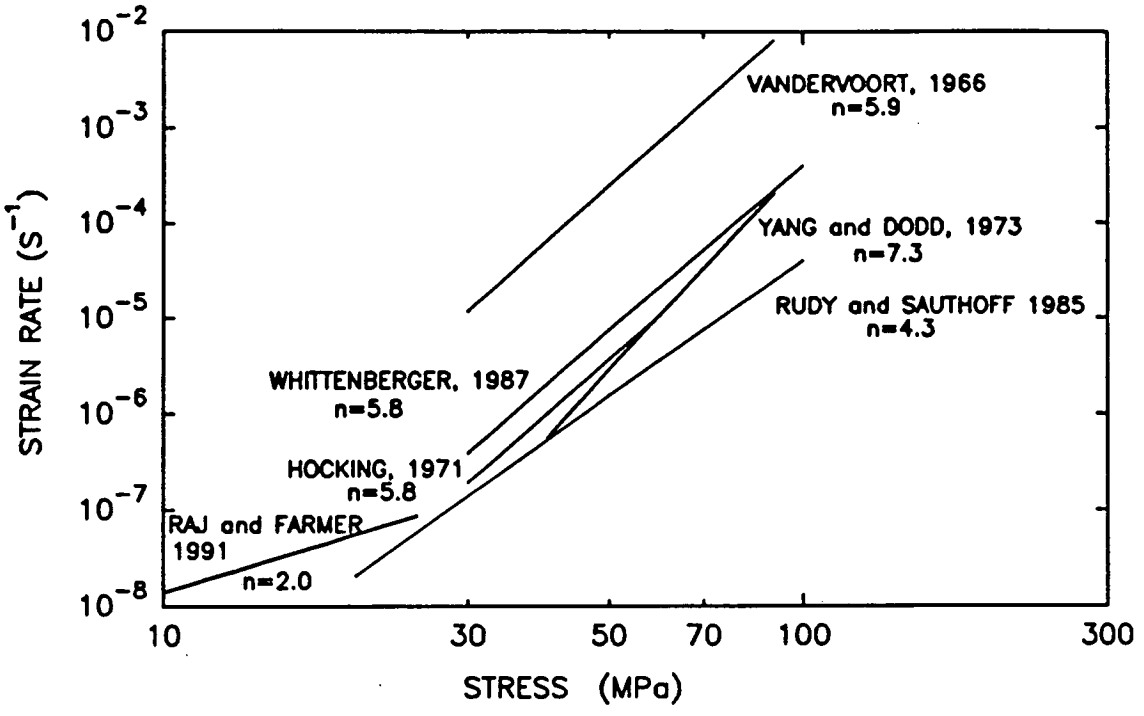

Figure 1. Compressive creep data for stoichiometric NiAl at 1175 K. Data are taken from refs. 11,14-16,18,33.

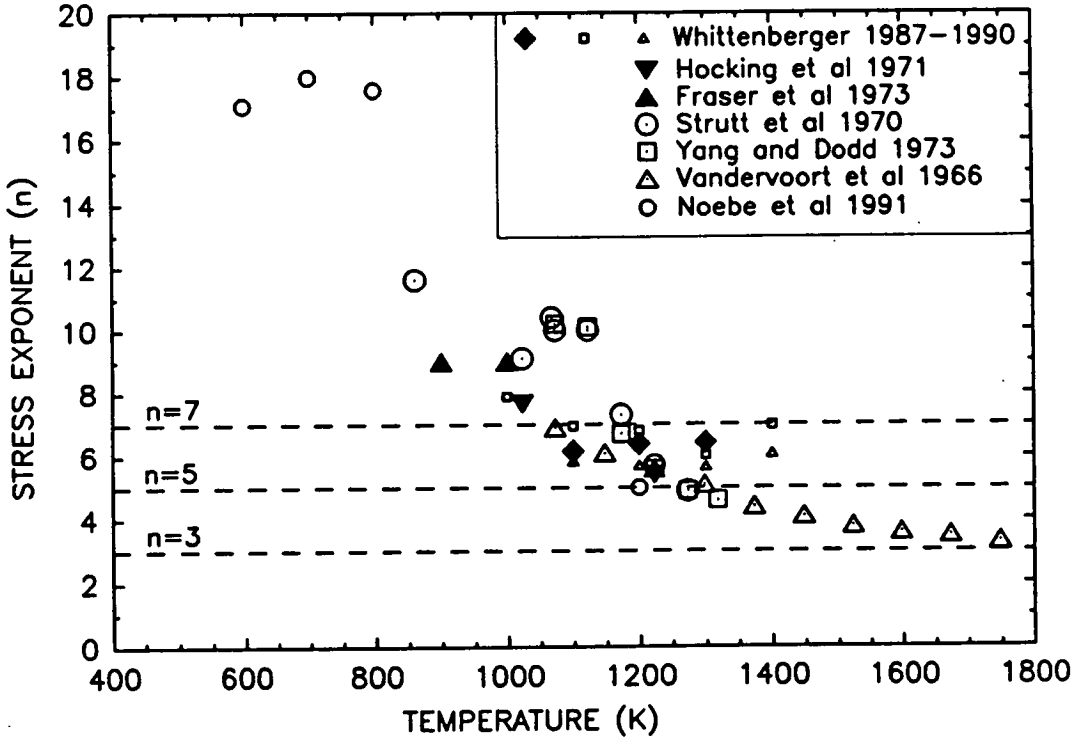

Figure 2. Temperature dependence of the stress exponent for stoichiometric NiAl. Data are taken from refs. 11-19,34.

the vast majority of results from a wide variety of sources indicate that high temperature creep in NiAl is climb controlled.

The 1300 K creep data for CoAl is summarized in Fig. 3. For this compound, the n values range between 2-5, which indicates a possible tendency towards Class A behavior. In fact, most of the data appear to show a transition from Class A to M between 1200 and 1400 K. At 1200 K, inverted primary creep(20,21,41), homogeneous dislocation structures(17, 41), and Class A response to strain rate changes(41) have been observed. In contrast, normal primary creep(20,41) and Class M response during strain rate changes(41) are observed at 1400 K. Dislocation structures during creep have not been reported, although subgrains have been observed after extrusion at ~1500 K(42). The fact that the stress exponent has not shown a corresponding increase at higher temperatures is probably the result of additional contributions to deformation by diffusional creep mechanisms.

FeAl also appears to creep by at least two different mechanisms, as shown in Fig. 4 and Table II. At high stresses and at temperatures below 1200-1300 K, the powder metallurgy materials studied by Whittenberger exhibit stress exponents which cluster near 6(23,44). In addition, normal primary creep is reported(23,44), but subgrains have not been observed(15,44). More conclusive determination of the mechanism(s) in this regime requires further experiments. At low stress levels at 1200 and 1300 K, and at higher temperatures, deformation appears to follow a stress exponent of 3-4(23). In this regime, normal primary creep was observed(23,43), but a lack of subgrains was again reported(43). The evidence of temperature dependent n values(23), a failure to reach the typical steady-state deformation conditions(23), observations of grain growth and dynamic recrystallization during deformation(23,45), and improved creep strength with coarser grain sizes(23) all lead to the conclusion that a superposition of both dislocation and grain boundary mechanisms are contributing to the creep response in this regime. Sauthoff and co-workers(15,43,46) have also observed such a transition in n values, although at a lower temperature, ~1025 K. Thus, the data from their studies in Fig. 4 show n ~4 at the same temperatures where the data of Whittenberger tend to display n ~6. Because their material was made by casting, grain boundary mobility is probably much higher than in the powder metallurgy material, which has oxide particles that restrict grain growth.

The next topic regarding creep of these compounds is the effect of stoichiometry. Fig. 5 is a plot of steady state creep rate at a given temperature and stress, as a function of Al content for all three B2 compounds. The testing temperatures indicated in the figure are approximately 70% of the absolute melting point, T_m. For NiAl, there is a broad range in composition ranging between about 45 and 52% Al, where the creep rate is roughly independent of composition. The largest difference in creep rates within this range of compositions is only a factor of 5. Only at very low Al contents is NiAl noticeably weaker(47, 48). This is most easily explained by the lower melting points of these compositions, which in turn implies a higher diffusivity, although the diffusivity data(24) would imply a more significant effect. These trends as a function of stoichiometry are reversed from those observed at lower temperatures(49), where defect hardening predominates over the effects of diffusion. As seen in Fig. 5, a much stronger dependence on stoichiometry is observed in CoAl, with the best creep strength close to the equiatomic composition. The creep behavior of FeAl follows that of the melting point, where a slight decrease in creep rate is observed as

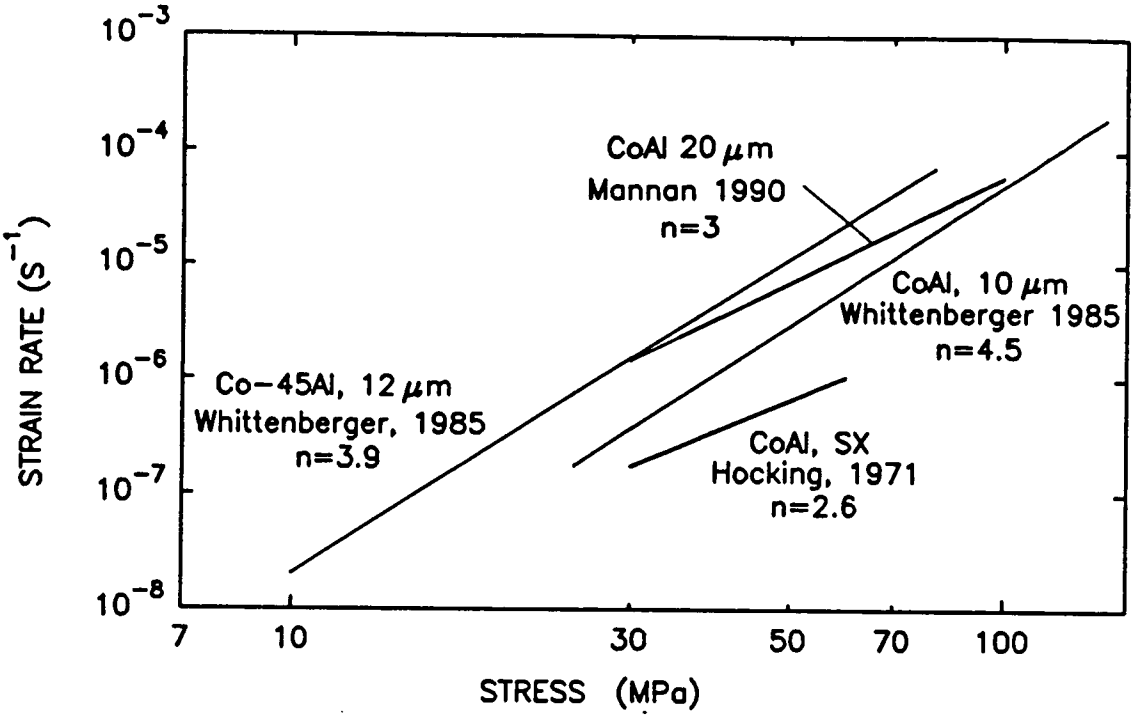

Figure 3. Compressive creep data for CoAl at 1300 K. Data are taken from refs. 17,20,21.

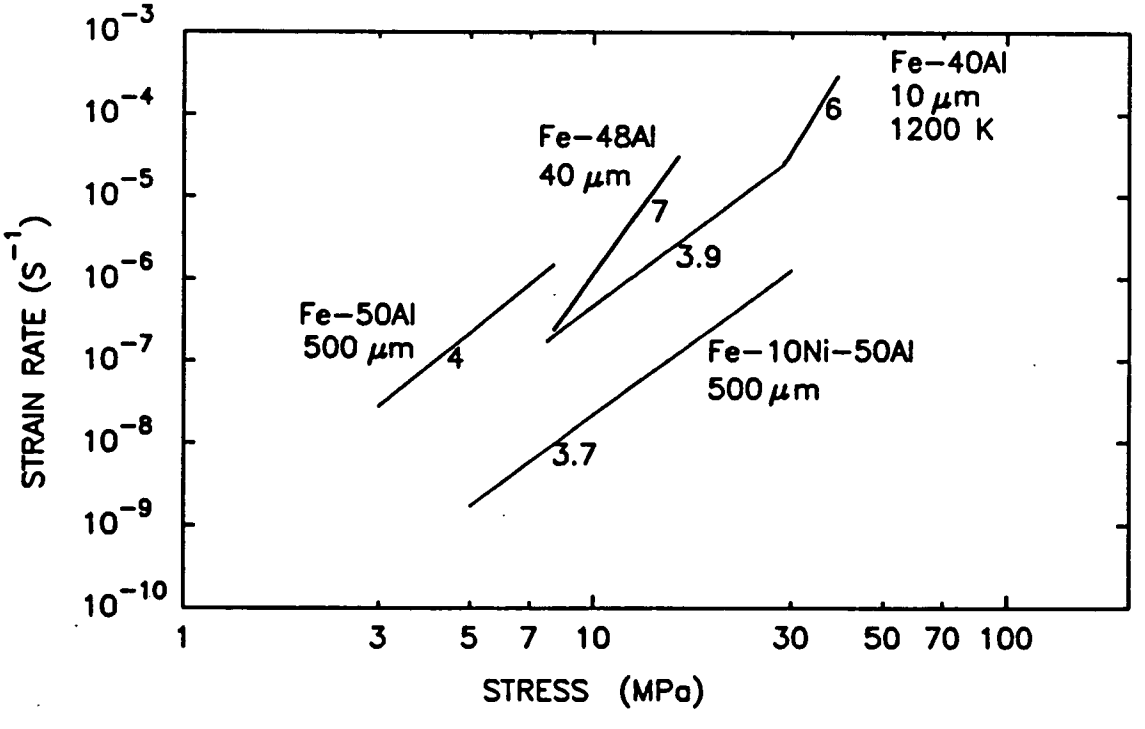

Figure 4. Compressive creep data for FeAl materials at 1175 K and Fe-40Al at 1200 K. Data are taken from refs. 15,23,43.

Al level is decreased. Diffusion data for FeAl also follow a weak dependence on Al content(28-30).

Although dislocation creep mechanisms are generally considered to be independent of grain size, studies of NiAl and FeAl have demonstrated that elevated temperature creep strength can sometimes be improved by decreasing the grain size. For example, Fig. 4 shows that the strength of the finer grained binary FeAl alloys is superior to the coarser grained forms, and such behavior was explained as a Hall-Petch effect (23). In the case of NiAl, the data in Fig. 6 illustrate that material with a grain size below ~10μm is capable of improved creep resistance. Since NiAl is a Class M material which exhibits subgrain boundaries that act as obstacles for dislocations, this behavior can be expected when the grain size is finer than the equilibrium subgrain size(11). Unfortunately, the effectiveness of fine grain size is restricted to lower temperatures and/or higher stresses, where diffusional creep mechanisms have less of an influence.

2.2 Diffusional Creep

Time dependent deformation can occur by stress assisted vacancy flow at stresses which are too low for dislocation processes to be significant. Creep by these diffusional mechanisms such as Nabarro-Herring or Coble creep is attributed solely to movement of vacancies from sources to sinks, which are usually grain boundaries of different orientations with respect to the applied stress. These mechanisms are characterized by stress exponents $n = 1$ and very strong dependencies on grain size, with large grained materials being more creep resistant. Rudy and Sauthoff(46) provided the most convincing evidence for diffusional mechanisms in a Ni-20Fe-50Al alloy, namely a stress exponent of 1. Additionally, there is some evidence in binary NiAl at temperatures above 1300 K and at low strain rates, where grain growth during the creep test resulted in coarser grained material having higher strengths(12). Fig. 1 also displays some new data generated by Raj and Farmer(33) showing a low stress exponent that may indicate some grain boundary assisted mechanism operating at low stresses. Despite these examples, the large body of literature regarding creep of NiAl provides little direct experimental support for creep by diffusional mechanisms over large regimes of temperature and stress. In fact, the calculated creep rates by this type of mechanism are much greater than the actual experimental data(50), implying that these mechanisms are suppressed compared to disordered metals. In Fig. 6, the fine grained material begins to lose its advantage at stresses below ~30 MPa, as the change in slope indicates. In general, the tendencies for diffusional creep mechanisms begin to become noticeable around 1300 K and are not really very strong until ~1400 K. As discussed in the previous section, evidence for diffusional mechanisms in FeAl and CoAl appear to commence at approximately $0.7T_m$ also.

Some qualifications should be mentioned with regard to the influence of grain size. The trends seen above are restricted to single phase materials that are relatively weak at these temperatures. If the resistance to dislocation creep is improved, for example by precipitation strengthening, then grain boundary effects may become more influential and coarse grained materials may be more desirable. Furthermore, since the majority of the creep data has been obtained by compression testing, grain boundary cavitation is rarely observed. Thus it is possible that different trends with grain size would be seen in

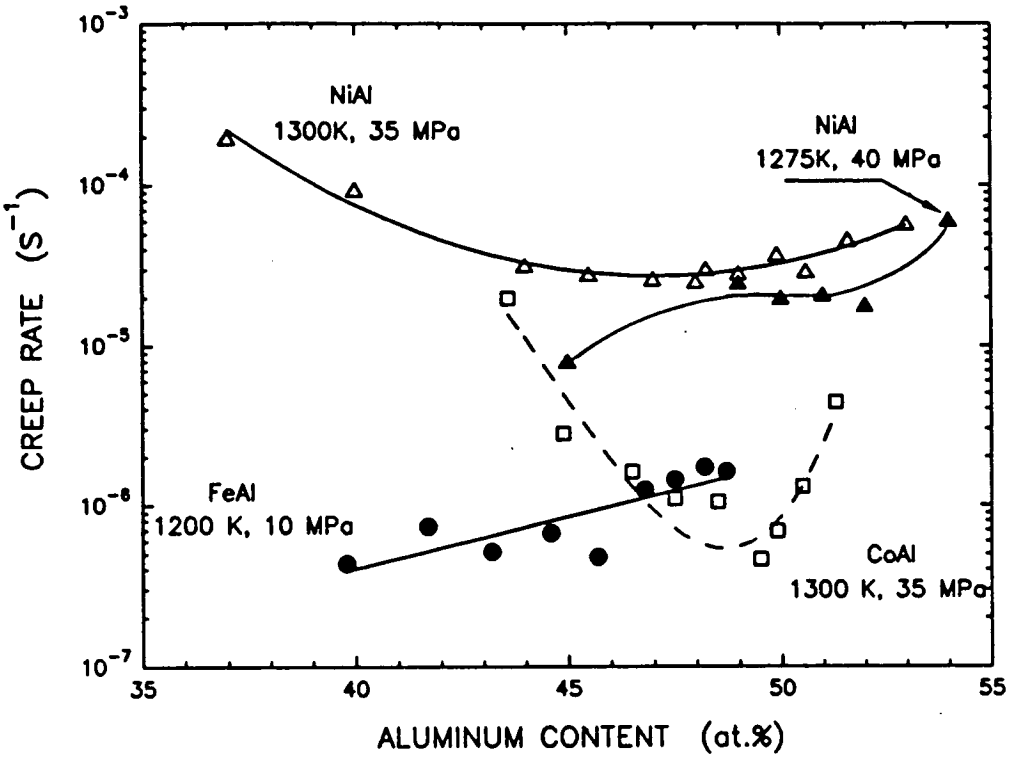

Figure 5. Creep rate as a function of stoichiometry for NiAl(12,14,47, 48), FeAl(23), and CoAl(20).

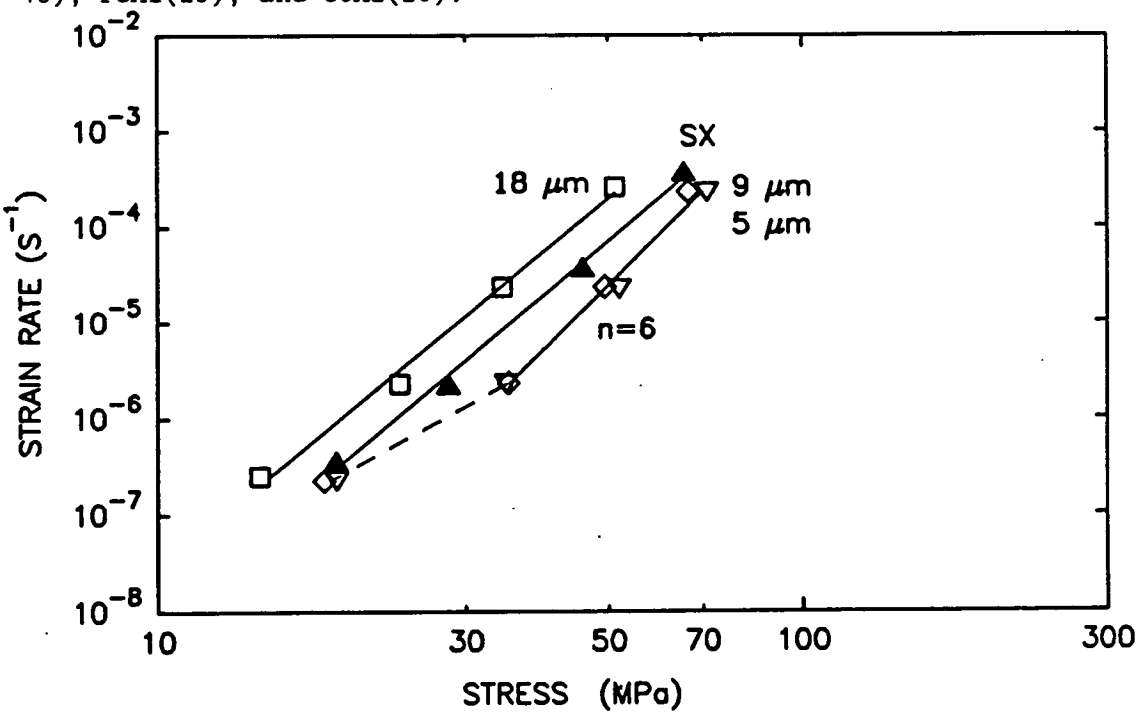

Figure 6. Compressive creep resistance as a function of grain size for NiAl at 1300K. Data are taken from refs. 11,19.

tension tests. One example of this is illustrated in Fig. 7 for FeAl. At 1100 K, the creep rates measured in tension and compression were in good agreement for binary Fe-40Al, but not for the alloy which was precipitate strengthened by Zr and B additions. This difference was traced to the onset of cavitation after a few percent strain in tension (51). Also note that the precipitate strengthened alloy had a 2-3 order of magnitude improvement in creep rate over the binary alloy in compression, but only a factor of 15 improvement in tension tests.

3. STRATEGIES FOR INCREASING CREEP RESISTANCE

This section considers various concepts for improving creep strength, primarily for NiAl. As an introduction, Fig. 8 is an example of how creep strength is built in a single crystal Ni-base superalloy (2). Starting with pure Ni, one can see that solid solution hardening with a heavy element such as W provides about 2 orders of magnitude improvement in creep rate. Creep data for a solid solution alloy that has a combination of Cr, Co, and W in a composition similar to that of the γ phase of the superalloy, follows the creep response of the Ni-2W binary. In other words, the effects of combining several solid solution elements are not additive. The presence of a long range ordered structure in Ni_3Al provides another 2 orders of magnitude improvement in creep rate, and solid solution hardening of Ni_3Al to form the composition of the γ' phase in the superalloy gives an additional factor of ten. However, the largest improvement in creep resistance, about a factor of 1000, is obtained by the superalloy with a two phase mixture of about 50% γ and γ'. So in total, there is a decrease of about 8 orders of magnitude in creep rate as progressive changes are made from pure Ni to the Ni-base superalloy, and the addition of a second phase is the major reason for this improvement.

Similar improvements are necessary for the aluminides to compete with current materials such as superalloys and Ni_3Al base alloys. Plots similar to Fig. 8 will be used for most of the comparisons of the various strengthening concepts which are discussed in the following sections. A rough criteria of success is obtained by judging how close the creep strength is to the superalloy, without compensating for the lower density of NiAl. Creep properties of the intermetallics, which were generated primarily in compression, will be compared to the tensile creep response of NASAIR 100, a first generation single crystal superalloy(52).

3.1 Solid Solution Strengthening

The role of solid solution hardening in NiAl is summarized in Fig. 9 at 1200 K, where the bulk of the data has been generated and the least amount of extrapolation was needed. Two data sets for binary NiAl are shown which cover the range in creep strength seen in the numerous studies, with both having a high stress exponent, n ~5. All of the solid solution alloys show some improvements in strength, but they also exhibit a change in n to a value near 3-4. Thus it appears that these solute additions change the creep mechanism to viscous drag behavior, in a manner very similar to that which occurs when alloying elements are added to pure metals. In fact, in one recent study(55), a transition from Class M to Class A behavior as a function of applied stress was observed, and the transition appeared to be well described by current theories developed for disordered solid solutions(6,7). However,

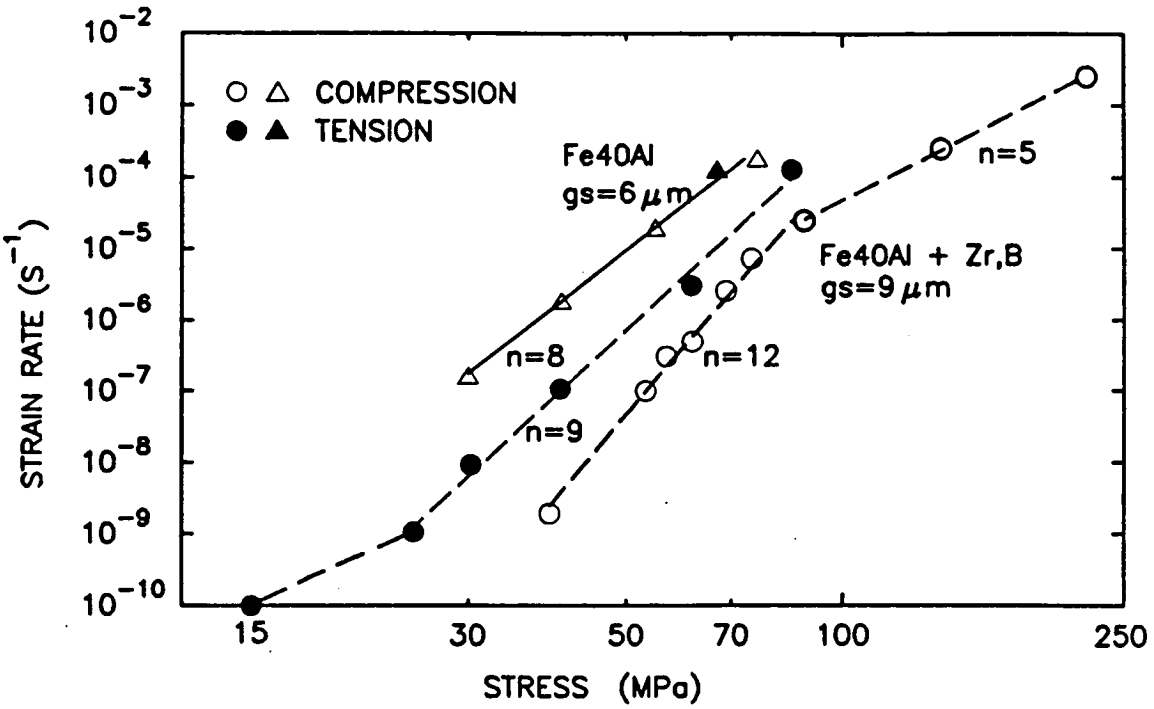

Figure 7. Comparison of creep response under tension and compression for Fe-40Al and Fe-40Al-0.1Zr-0.5B at 1100 K (51).

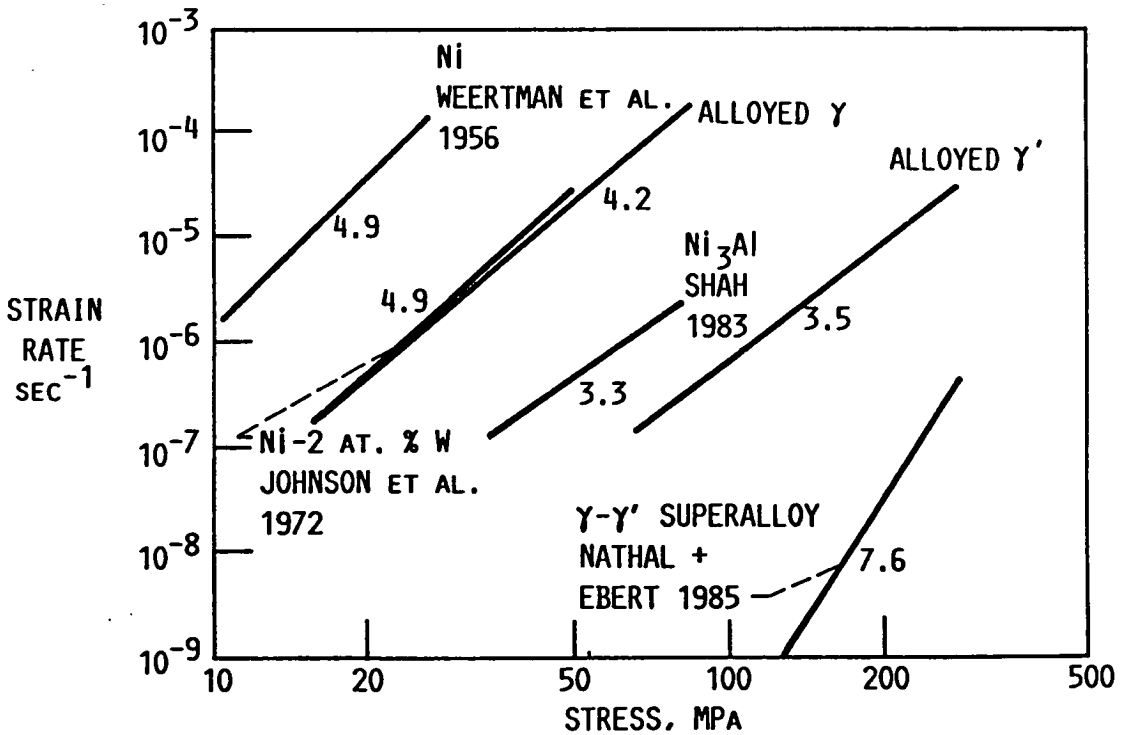

Figure 8. Building creep strength at 1275 K in steps from pure Ni to a Ni-base superalloy(2).

because of this new stress exponent, the strength improvements over the binary are only large at high stresses, and in the lower stress regime the advantage is reduced or eliminated. Finally, it is of interest to note in Fig. 9 that one of the largest strengthening effects was produced by an addition of only 0.05 at.% Zr. This sensitivity to small differences in composition might be the main reason for discrepancies in mechanical properties among various published results. Fig. 4 shows data for FeAl that indicate significant improvements in creep resistance with solid solution additions of Ni. Solid solution hardening of CoAl by Fe and Ni has also been reported(56). Since both of these binary compounds have tendencies towards Class A behavior, it would not be surprising that the ternary alloys would also show similar trends. In summary, it appears that solid solution hardening does provide some creep strength improvements over the binary compounds, but this concept is inadequate by itself and must eventually be used in combination with other strengthening mechanisms.

3.2 Precipitation Strengthening

Significant improvements in creep strength of NiAl by precipitation hardening were first demonstrated by Polvani et al.(57) by adding Ti to form a two phase mixture of NiAl and Heusler phase Ni_2AlTi. Similar Heusler phases and other phases such as Laves (eg., NiAlTa) can be formed with many ternary additions such as Nb, Ta, Hf and V. The creep properties of some Ti and Ta containing alloys are presented in Fig. 10, where it is evident that these materials are reasonably strong, but again, extrapolation to low stresses shows the advantages diminishing. The reasons for the low stress exponent in these alloys is not entirely clear, since most creep resistant, two-phase alloys exhibit significantly higher stress exponents than the matrix phase. In most cases, the microstructures of the ternary alloys were probably not optimized: for example if the second phase is not fine enough, effective strengthening would not be expected. Equally valid explanations may be that the observed n values represent a superposition of several deformation mechanisms, including diffusional creep, and/or that coarsening of the precipitate phase results in less strengthening in the low stress/long life regime. TEM micrographs of the Ti-rich Heusler phase containing alloys after creep testing(53,57) exhibit semi-coherent β-β' interfaces which are reminiscent of microstructures in γ-γ' superalloys(52). Again, by analogy to the superalloys, optimizing the creep strength requires a balance of the compositions of the two phases, the precipitate volume fraction, the size and distribution of the precipitates. The use of single crystal technology would also seem necessary in order to realize the full benefits of the precipitates. In fact, Darolia(58) has recently reported promising tensile creep-rupture properties for single crystals containing Heusler precipitates.

Another example of the sensitivity of creep strength to microstructure in these alloys is shown in Fig. 11. The alloys with Nb-rich Laves phase behave similarly to the other alloys in Fig. 10, but it is also evident that by changing the processing of the same alloy from cast and extrusion to directional solidification, both the creep strength and the stress exponent were changed. It is also important to note that the directionally solidified material was not optimized, since the second phase was only partially aligned(60). Other options involving precipitation hardening also exist, such as the use of different phases which may have better strengthening or microstructural

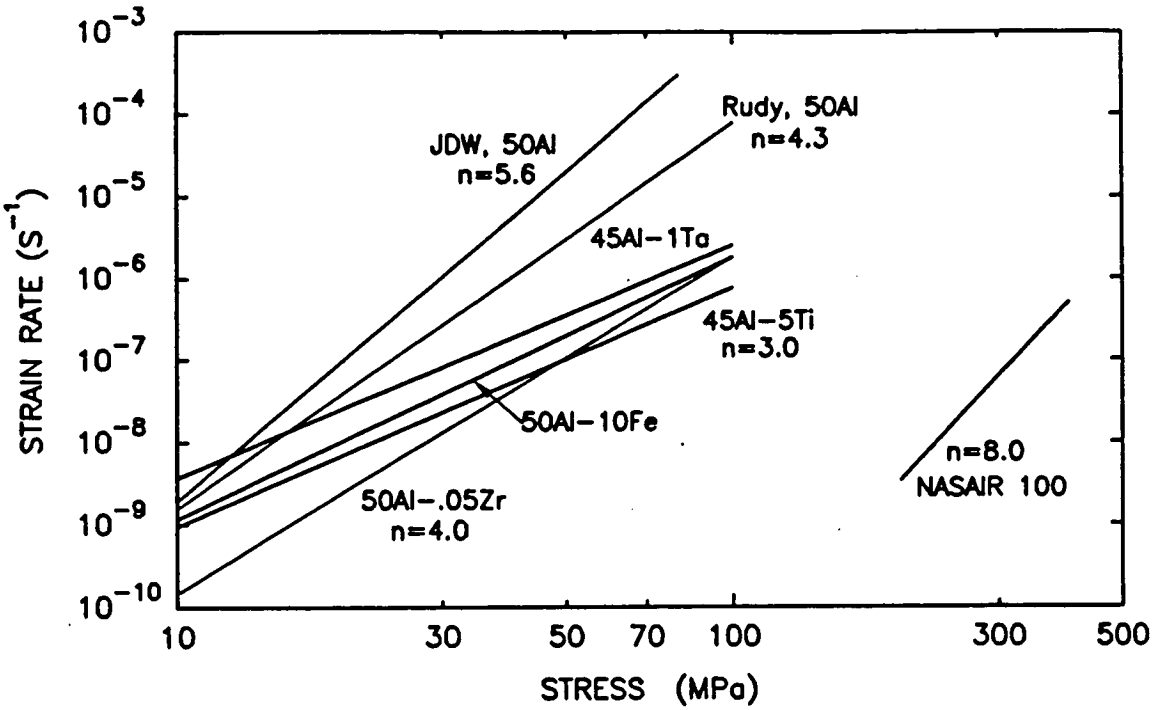

Figure 9. Solid solution hardening of polycrystalline NiAl in compressive creep at 1200 K. Data are taken from refs. 12,15,19,46,52-54.

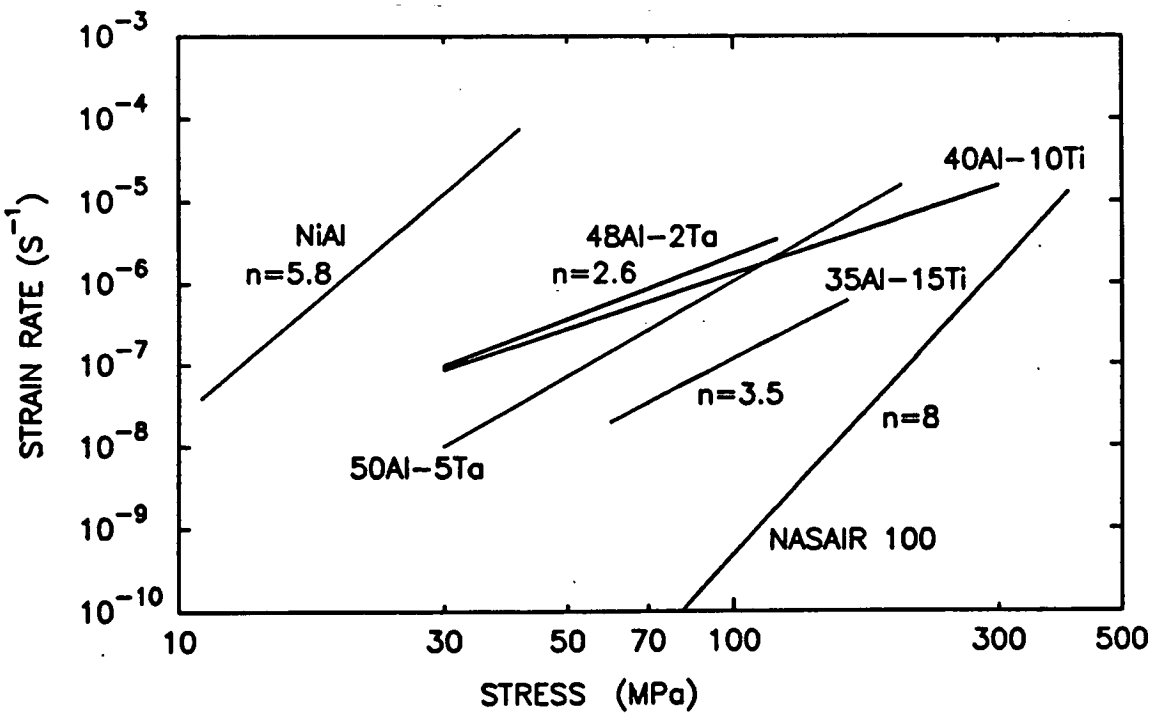

Figure 10. Precipitation hardening of NiAl by Heusler and Laves phases in compressive creep at 1300 K. Data are taken from refs. 12,52-54,57.

stability characteristics(61).

3.3 Dispersion Strengthening

This section addresses the use of rapid solidification to add fine dispersoids. This concept takes advantage of the fact that many elements or compounds are soluble in liquid NiAl but insoluble in the solid. By rapid solidification, very fine dispersions of second phases, with diameters on the order of 20-50 nm, can form that are resistant to coarsening due to the very low solubility. For NiAl, both pure elements such as W and Mo and various carbides or borides are candidates for this type of strategy. These dispersoids also tend to pin grain boundaries and result in significant grain refinement(62-64). Fig. 12 reveals that the additions of pure W(64) and TiC(62) had very little strengthening effect, and TiB_2(62) showed about an order of magnitude improvement over binary NiAl. However, this degree of strengthening can be achieved simply due to grain refinement similar to that shown in Fig. 6, so dispersoid/dislocation interactions are not expected for these alloys.

More interesting are the improvements achieved with HfB_2(65) and HfC(62,63), which are both considerably stronger than binary NiAl. In the case of HfC there was some indication of a threshold stress at ~50 MPa below which no creep occurs(63). However, more recent work has shown that this apparent threshold stress is the result of dynamic grain growth which is a function of testing conditions(4). These new data indicate that for HfC strengthened NiAl, coarse grained material is more creep resistant than the finer grained product, which is the opposite of the trends observed in the binary. Thus the grain interiors have been strengthened sufficiently such that diffusional creep mechanisms are occurring at similar rates. The mechanism for the improved strength are related primarily to the interaction of the dispersoids with mobile dislocations(62,63) and subgrain boundaries(65). However, it is probably not a coincidence that the two most effective dispersoids contained Hf, and it is quite possible that small amounts of Hf in solution could strengthen NiAl in a manner similar to that observed in Fig. 9 for small Zr additions.

In summary, the use of rapid solidification to dispersion strengthen NiAl has not yet provided sufficient strengthening to compete effectively with superalloys. The potential for improvement exists, primarily in the areas of optimizing the dispersoid volume fractions, and in devising the thermo-mechanical processing schedules needed to produce the desired grain structures that have proven successful in the oxide dispersion strengthened Ni-base alloys(66).

In FeAl, strengthening by additions of Fe_6Al_6Zr and ZrB_2 particles has been demonstrated at temperatures up to 1100 K(51,67), as was seen in Fig 7. Additional strengthening by Y_2O_3 dispersoids has also been observed(68). However, the relative contributions to creep strength from elements in solid solution, precipitates, dispersoids, and grain refinement remain uncertain.

3.4 Reaction Milled Composites

An unusual example of a composite is the AlN dispersoid-reinforced NiAl which was produced by reaction milling in liquid nitrogen(69,70). This process produces very fine dispersoids, on the order of 20-50 nm, at relatively high volume fractions of ~10%. These particles are not uniformly distributed, but are clustered along prior particle

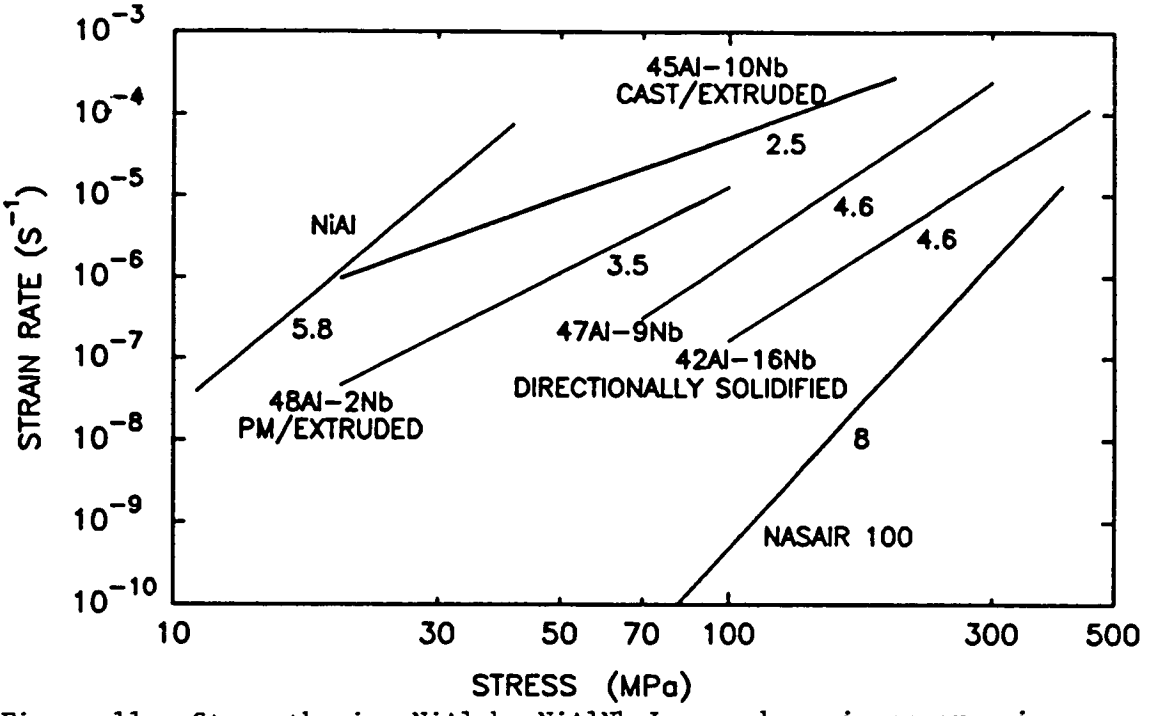

Figure 11. Strengthening NiAl by NiAlNb Laves phase in compressive creep at 1300 K, showing the effect of variations in microstructure. Data are taken from refs. 12,52,54,59,60.

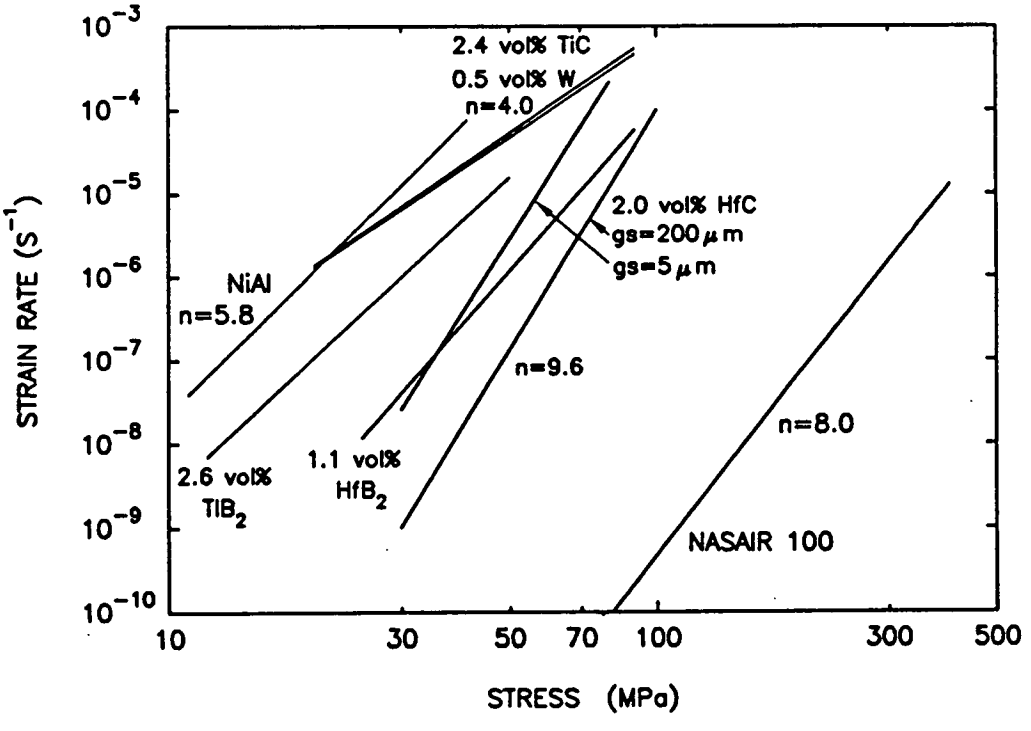

Figure 12. Effect of dispersoids added by rapid solidification techniques on compressive creep of NiAl at 1300 K. Data are taken from refs. 4,12,52,62,63,65.

boundaries. The properties of this material are very promising, since as seen in Fig. 13, creep strengths approaching that of NASAIR 100 were obtained. After correcting for density, the deformation resistance of the superalloy and AlN/NiAl are actually equivalent. Also of interest is that the properties of extruded material, where the particle-rich regions are strung out along the extrusion direction, were roughly equivalent to HIP-consolidated material, where the particles are not aligned but still segregated. The reasons for the exceptional properties of this type of second phase reinforcement are not currently understood, although the promising results in compression certainly warrant more extensive testing in tension.

3.5 Discontinuous Reinforced Composites

Another approach to strengthening is through the use of composites with discontinuous reinforcements. These reinforcements are typically larger in size and present in higher concentrations than that found in dispersion strengthened materials. One example is TiB_2 particulate reinforced NiAl, where composites with 1μm diameter particles were produced by an exothermic reaction process(13). Fig. 14 reveals that composites made in this manner do show improvements in strength that scale with the amount of reinforcement. It is important to note that the stress exponents are all high, which leads to a creep strength advantage that is maintained or improved at lower stresses. When the stress exponent is increased, it usually indicates that the dislocation substructure is refined and stabilized by the second phase when compared to the same matrix without the reinforcement. Evidence for this has been provided by transmission electron microscopy(13), where the creep deformation structure was characterized by subgrain boundaries which are usually pinned by the particles, in combination with a much higher dislocation content within the subgrains. It is clear that the TiB_2 particles are effective in stabilizing a higher dislocation density which results in the observed strengthening.

Similar strength improvements have been observed when TiB_2 particles were added to CoAl(21). However, an attempt at combined strengthening from both Heusler precipitates and TiB_2 particles was unsuccessful(53).

Another type of discontinuous reinforcement which has been produced in NiAl is Al_2O_3 whiskers(71). The whiskers, which had an average aspect ratio of approximately 7.5, were added by mechanical blending at volume fractions ranging up to 25%. The mechanical properties from those composites are presented in Fig. 15. Some improvements in creep resistance are seen, but the whiskers are not as effective as the TiB_2 particles described above. Also of interest is that the stress exponents of the composites were the same as that of the matrix, which indicates that deformation is controlled by flow in the matrix, as predicted by several models of composite strengthening(72). These models would predict further improvements in creep strength by increasing the aspect ratio of the whiskers. However, because some whisker breakage after testing was observed, higher strength whiskers will also be needed. Control of whisker distribution and alignment, and whisker damage during processing, are generally major problems in this type of composite. Finally, hybrid composites containing both TiB_2 particulates and Al_2O_3 whiskers have been made and have shown that these strengthening concepts were additive.

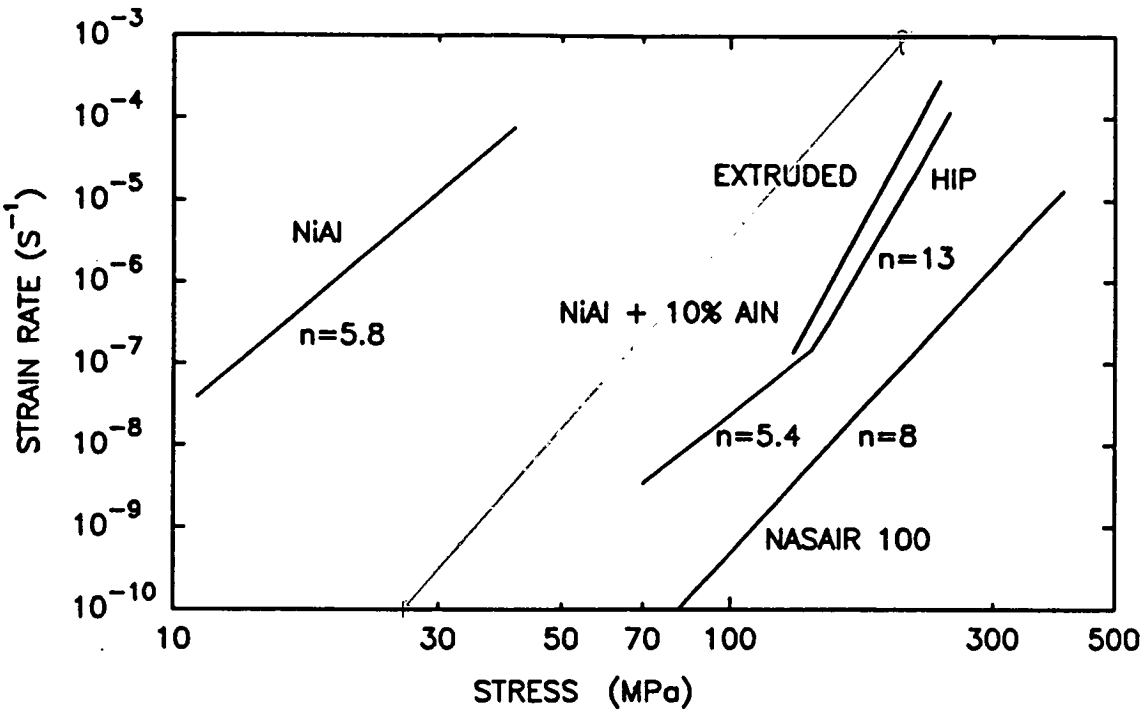

Figure 13. Effect of AlN dispersoids added by a reaction milling process on compressive creep of NiAl at 1300 K. Data are taken from refs. 12,52,69,70.

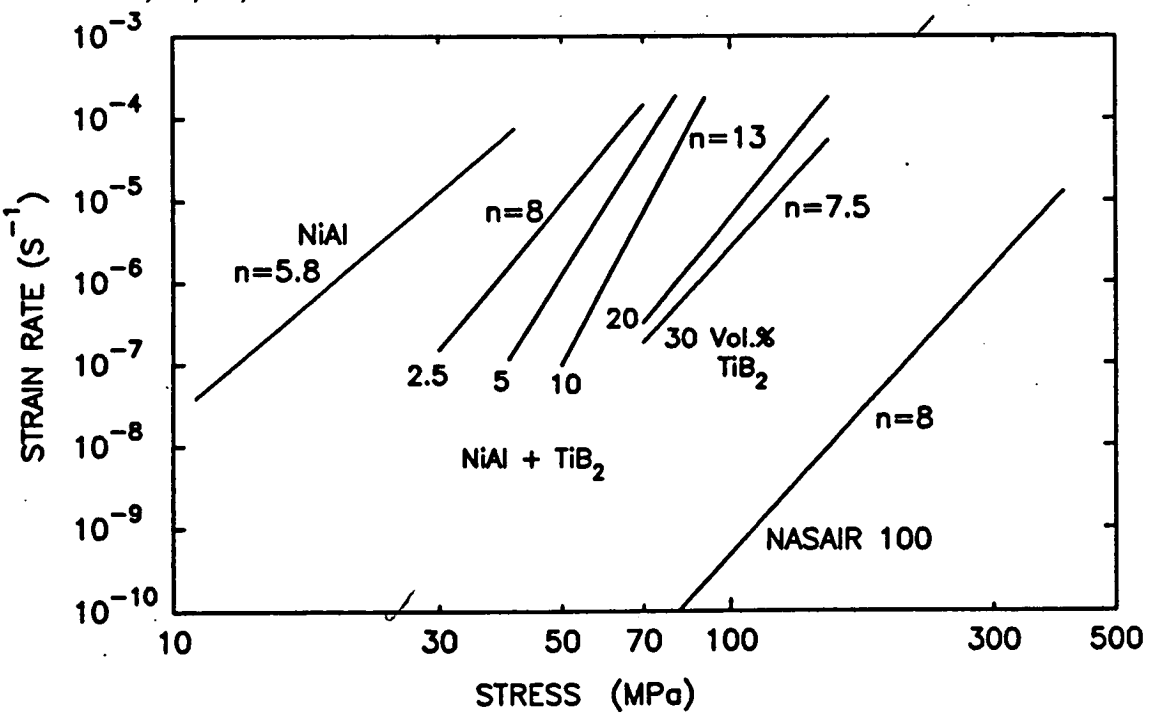

Figure 14. Effect of TiB_2 particles added by exothermic reaction synthesis on compressive creep of NiAl at 1300 K. Data are taken from refs. 12,13,52.

3.6 Continuous Reinforcement Composites

The final strategy to discuss is the reinforcement of NiAl with continuous fibers. Such composites can either be natural, such as directionally solidified eutectics, or artificially fabricated, in order to use fiber-matrix combinations not achievable through eutectic solidification. The early work by Walter and Cline(73) has shown that a eutectic consisting of α-Cr rods in a NiAl matrix possessed some very promising creep properties, as indicated in Fig. 16. Similar eutectic microstructures can be produced with Mo(74), W(64), Re(75), and NiAlNb (60) phases, and these may also prove to be advantageous.

Some artificial composites have been made by a powder metallurgy approach of hot pressing matrix powders around either W or Al_2O_3 fibers and have been tested in bending(76). There were substantial strength improvements in the W/NiAl system over the stand-alone matrix, whereas the Al_2O_3/NiAl composites did not show any strengthening. This was traceable to different degrees of bonding, where load could be transferred to the strongly bonded W fibers but not to the weakly bonded Al_2O_3. However, the composite with weakly bonded fibers did show evidence of toughening, and thus a hybrid concept of using two types of reinforcement is one way to achieve a balance of properties. Further testing of these composites is required to ascertain whether the high strengths will be maintained in creep tests, and whether they can survive in an environment involving thermal cycling.

4.0 SUMMARY

High temperature creep deformation in NiAl appears to be satisfactorily described by pure metal type, or dislocation climb controlled creep, as all of the major defining characteristics of this class of creep have been observed. Stoichiometry variations appear to be relatively unimportant, especially between 45 and 52 % Al, a fact which is surprising based on the relatively large effect of stoichiometry on diffusion characteristics. Diffusional creep mechanisms appear to become important at low stresses and above about 0.7Tm, although they appear to be more prominent in ternary alloys and in materials which have been strengthened against dislocation creep. CoAl has exhibited mixtures of both climb and glide controlled behavior, and may in fact undergo a transition from Class A to M as temperature increases. Creep in CoAl is much more dependent on stoichiometry, with a maximum in creep strength seen near 50% Al. FeAl has also shown intermediate behavior with a mixture of both Class A and M traits, and exhibits the opposite effect of being more creep resistant at substoichiometric Al levels. Both CoAl and FeAl have shown larger contributions from diffusional creep mechanisms that appear to be acting concurrently with dislocation creep. Of the three aluminides, only FeAl has exhibited an activation energy significantly higher than that for diffusion. An additional note of importance is the heavy reliance on compression testing that exists in the literature. Compression tests are very valuable in isolating deformation mechanisms and for providing an indication of the maximum creep strength achievable in a given material. However, several technologically important topics such as grain boundary cavitation, necking, and tertiary creep can best be examined in tension creep experiments.

The various strategies to improve the creep resistance of NiAl are summarized in Table III, along with suggested areas for future work

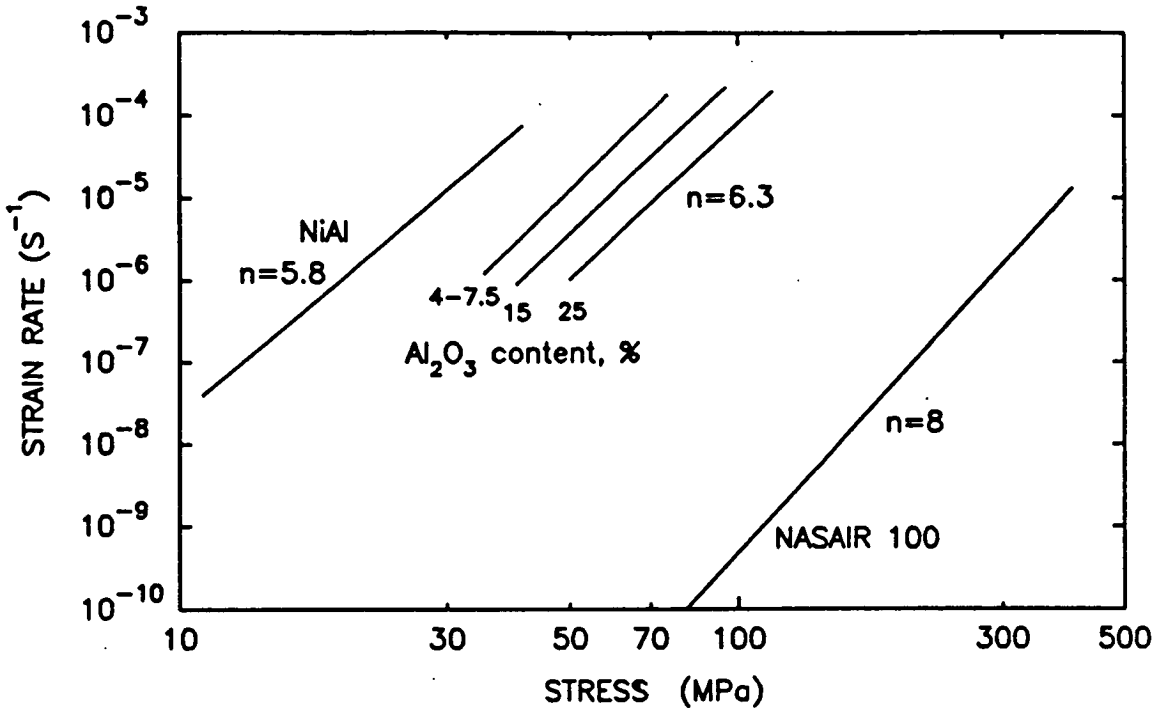

Figure 15. Effect of Al_2O_3 whiskers added by a mechanical blending on compressive creep of NiAl at 1300 K. Data are taken from refs. 12,52,71

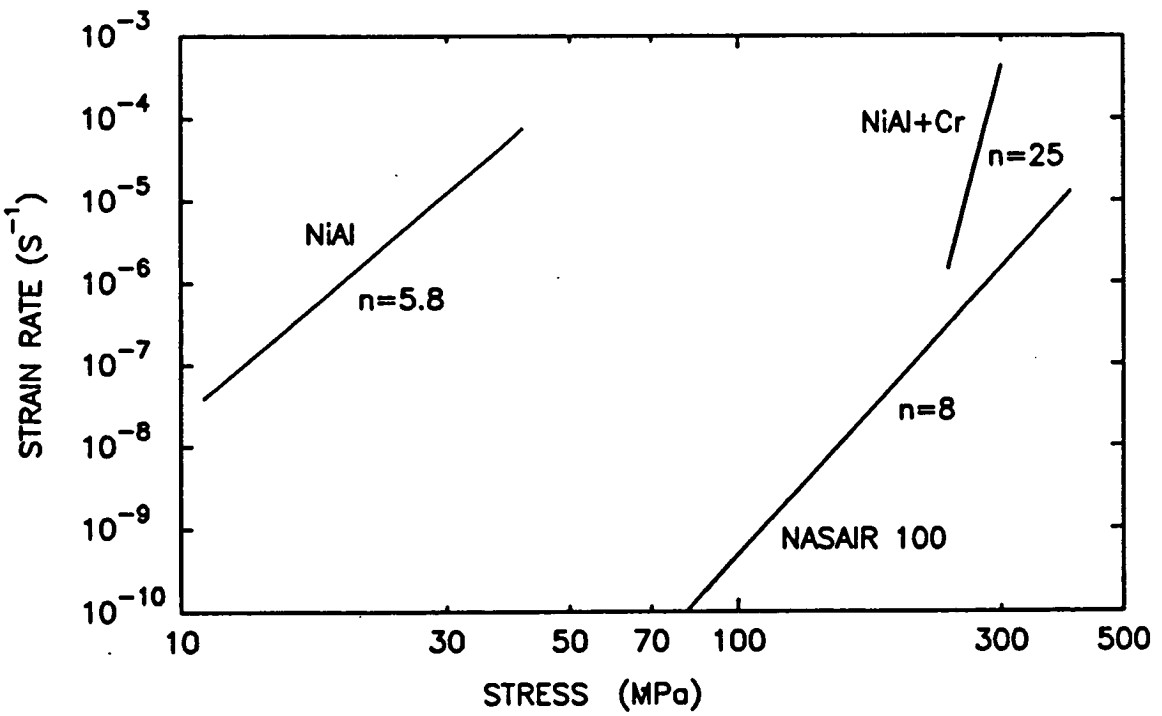

Figure 16. Tensile creep of directionally solidified NiAl-34Cr eutectic at 1300 K. Data are taken from refs. 12,52,73.

aimed at further improvements. Of these attempts, both solid solution and precipitation hardening have shown progress, but the low stress exponents of these materials results in less attractive properties at lower stresses and creep rates. However, recent advances using precipitate strengthening in single crystals have shown some very good promise. Rapid solidification has shown only small improvements in strength, whereas TiB_2 particulates and Al_2O_3 whiskers showed larger but still insufficient advances. The AlN/NiAl composite has some of the best creep properties to date, comparable to the Cr containing directionally solidified eutectic. Finally, the strengthening which can be achieved with continuous fibers is dependent on the choice of the fiber and the bonding with the matrix.

In most of the above strategies, options exist for exploring further improvements in creep strength. New types of precipitates or other reinforcements in combination with microstructural control may produce more significant results. Furthermore it is important to acknowledge that a balance of properties is required for most applications, and low temperature toughness, density, environmental resistance, fabricability and cost must eventually be considered.

TABLE III
Strategies For Improving Creep Strength of NiAl

STRATEGY	CURRENT STATUS	SUGGESTED MEANS OF IMPROVEMENT
Solid Solution + Precipitates	Limited benefits in low ϵ regime	Single crystal + possible new phases
Dispersoids by RST	Only small improvements in strength	New vol. % + mechanical working
AlN Dispersoids	Largest strengthening to date	Processing
Particulates	TiB_2 significant benefit but not enough	Hybrid composites
Whiskers	Al_2O_3 small benefit	Whisker availability + alignment, processing
D.S. Eutectics	Large strengthening with Cr	
Continuous Fibers	Potential strengthening but dependent on fiber and bonding	Fiber availability

5.0 REFERENCES

1. W.D. Nix and B. Ilschner, in 5th Int. Conf. Strength of Metals and Alloys, ed. by P. Hassen et al., Pergamon Press, 3, p. 1503 (1980).

2. M.V. Nathal, J.O. Diaz, and R.V. Miner, in High Temperature Ordered Intermetallic Alloys III, Proc. MRS, ed. by C.T. Liu et al., 133, p. 269 (1989).
3. W.C. Oliver and W.D. Nix, Acta Metall., 30, p. 1335 (1982).
4. J.D. Whittenberger, R. Ray, and S.C. Jha, in High Temperature Ordered Intermetallic Alloys IV, Proc. MRS, ed. by L.A. Johnson et al., 213, p. 581 (1991).
5. M.J. Mills, J.C. Gibeling and W.D. Nix, Acta Metall., 34, p. 915, (1986).
6. F.A. Mohamed and T.G. Langdon, Acta Metall., 22, p. 779 (1974).
7. M.S. Soliman and F.A. Mohamed, Mat. Sci. Eng., 55, p. 111 (1982).
8. A.M. Mukherjee, J.E. Bird, and J.E. Dorn, Trans. ASM, 62, p. 155 (1969).
9. D.L. Yaney, J.C. Gibeling and W.D. Nix, Acta Metall., 35, p. 1391 (1987).
10. T.G. Langdon and P. Yavari, in Creep and Fracture of Engineering Materials and Structures, ed. by B. Wilshire and D.R.J. Owen, Pineridge Press, Swansea, UK, p. 71 (1981).
11. J.D. Whittenberger, J. Mat. Sci., 23, p. 235 (1988).
12. J.D. Whittenberger, J. Mat. Sci., 22, p. 394 (1987).
13. J.D. Whittenberger, R.K. Viswanadham, S.K. Mannan, and B. Sprissler, J. Mat. Sci., 25, p. 35 (1990).
14. W.J. Yang and R.A. Dodd, Met. Sci. J., 7, p. 41 (1973).
15. M. Rudy and G. Sauthoff, in High-Temperature Ordered Intermetallic Alloys, Proc. MRS, ed. by C.C. Koch et al., 39, p. 327 (1985).
16. R.R. Vandervoort, A.K. Murkerjee, and J.E. Dorn, Trans. ASM, 59, p. 930 (1966).
17. L.A. Hocking, P.R. Strutt, and R.A. Dodd, J. Inst. Metals, 99, p. 98 (1971).
18. J. Bevk, R.A. Dodd, and P.R. Strutt, Met. Trans., 4, p. 159 (1973).
19. R.D. Noebe and J.D. Whittenberger, unpublished research, NASA-Lewis Research Center, Cleveland, OH (1991).
20. J.D. Whittenberger, Mat. Sci. Eng., 73, p. 87 (1985).
21. S.K. Mannan, K.S. Kumar, and J.D. Whittenberger, Metall. Trans., 21A, p. 2179 (1990).
22. A. Lawley, J.A. Coll, and R.W. Cahn, Trans. ASM, 218, p. 166 (1960).
23. J.D. Whittenberger, Mat. Sci. Eng., 77, p. 103 (1986).
24. G.F. Hancock and B.R. McDonnell, Phys. Stat. Sol., 4(a), p. 143 (1971).
25. A. Lutze-Birk and H. Jacobi, Scripta Metall., 9, p. 761 (1975).
26. S. Shankar and L.L. Seige, Metall. Trans, 9A, p. 1467 (1978).
27. A.E. Berkowitz, F.E. Jaumot, and F.C. Nix, Phys. Rev., 95, p. 1185 (1954).
28. H.C. Hagel, in Intermetallic Compounds, ed. by J.H. Westbrook, p. 377 (1977).
29. K. Hirano and A. Hishinuma, Nippon Kinzoku Gakkaishi, 32, p. 516 (1968); Diffus. Data, 3, p. 270 (1969).
30. K. Nishida, T. Yamamoto, and T. Nagata, Nippon Kinzoku Gakkaishi, 34, p. 591 (1970); Diffus. Data, 5, p. 26 (1971).
31. M.R. Harmouche and A. Wolfenden, Mat. Sci. Eng., 84, p. 35 (1986).
32. M.R. Harmouche and A. Wolfenden, J. Testing and Evaluation, 15, p. 101 (1987).
33. S.V. Raj and S. Farmer, unpublished research, NASA-Lewis Research Center, Cleveland, OH (1991).
34. H.L. Fraser, R.E. Smallman, and M.H. Loretto, Phil. Mag., 28, p. 651 (1973).

35. M.F. Ashby, Acta Metall., 20, p. 887 (1971).
36. J.E. Bird, A.K. Mukherjee, and J.E. Dorn, in Int. Conf. Quantitative Relation Between Properties and Microstructure, ed. by D.G. Brandon and A. Rosen, Israel Univ. Press, p. 255 (1969).
37. A. Ball and R.E. Smallman, Acta Metall., 14, p. 1517 (1966).
38. E.P. Lautenschlager, T.C. Tisone, and J.O. Brittain, Phys. Stat. Sol., 20, p. 443 (1967).
39. P.R. Strutt, R.A. Dodd, and G.M. Rowe, in 2nd Int'l. Conf. Metals and Alloys, ASM, Metals Park, OH, III, p. 1057 (1971).
40. W.R. Kanne Jr., R.R. Strutt, and R.A. Dodd, Trans. AIME, 245, p. 1259 (1969).
41. D.L. Yaney and W.D. Nix, J. Mat. Sci., 23, p. 3088 (1988).
42. D.L. Yaney, A.R. Pelton, and W.D. Nix, J. Mat. Sci., 21, p. 2083 (1986).
43. M. Rudy and G. Sauthoff, Mat. Sci. Eng., 81, p. 525 (1986).
44. J.D. Whittenberger, Mat. Sci. Eng., 57, p. 77 (1983).
45. I. Baker and D.J. Gaydosh, Metallography, 20, p. 347 (1987).
46. I. Jung, M. Rudy, and G. Sauthoff, in High-Temperature Ordered Intermetallic Alloys II, Proc. MRS, ed. by N.S. Stoloff et al., 81, p. 263 (1987).
47. J.D. Whittenberger, R.D. Noebe, C.L. Cullers, K.S. Kumar, and S.K. Mannan, Metall. Trans., in press (1991).
48. J.D. Whittenberger, K.S. Kumar, and S. K. Mannan, J. Mat. Sci., 26, p. 2015 (1991).
49. R.T. Pascoe and C.W.A. Newey, Met. Sci. J., 2, p. 138 (1968).
50. J.D. Whittenberger, NASA-TM 101382 (1987).
51. J.D. Whittenberger, D.J. Gaydosh, and M.V. Nathal, unpublished research, NASA-Lewis Research Center, Cleveland, OH (1991).
52. M.V. Nathal and L.J. Ebert, Metall. Trans., 16A, p. 1863 (1985).
53. J.D. Whittenberger, R.K. Viswanadham, S.K. Mannan, and S.K. Kumar, J. Mat. Res., 4, p. 1164 (1989).
54. V.M. Pathare, PhD Thesis, Case Western Reserve University, Cleveland, OH (1987); NASA CR-182113 (1988).
55. S.V. Raj, I.E. Locci, and R.D. Noebe, unpublished research, NASA-Lewis Research Center, Cleveland, OH (1991).
56. J.D. Whittenberger, Mat. Sci. Eng., 85, p. 91 (1987).
57. R.S. Polvani, W.S. Tzeng, and P.R. Strutt, Metall. Trans., 7A, p. 33 (1976).
58. R. Darolia, J. Metals, 43, no. 3, p. 44 (1991).
59. J.D. Whittenberger, L.J. Westfall, and M.V. Nathal, Scripta Metall., 23, p. 2127 (1989).
60. B. Oliver, R.D. Noebe, and J.D. Whittenberger, unpublished research, Univ. of Tennessee, Knoxville, TN (1991).
61. I.E. Locci, R.D. Noebe, R.R. Bowman, R.V. Miner, M.V. Nathal, and R. Darolia, in High Temperature Ordered Intermetallic Alloys IV, Proc. MRS, ed. by L.A. Johnson et al., 213, p. 1013 (1991).
62. J.D. Whittenberger, D.J. Gaydosh, and K.S. Kumar, J. Mat. Sci., 25, p. 2771 (1990).
63. S.C. Jha, R. Ray, and J.D. Whittenberger, Mat. Sci. Eng., A119, p. 103 (1989).
64. I.E. Locci, R.D. Noebe, J.A. Moser, D.S. Lee, and M.V. Nathal, in High Temperature Ordered Intermetallic Alloys III, Proc. MRS, ed. by C.T. Liu et al., 133, p. 639 (1989).
65. J.D. Whittenberger, R. Ray, S. Jha, and S.L. Draper, Met. Sci. Eng., in press (1991).
66. R.C. Benn, in MiCon 86: Optimization of Processing, Properties, and

Service Performance through Microstructural Control, ed. by B.L. Bramfitt et al., ASTM STP 979, p. 238 (1988).
67. M.A. Morris and D.G. Morris, Acta Metall. Mater., 38, p. 551 (1990).
68. S. Struthers, PhD Thesis, Case Western Reserve University, Cleveland, OH (1991).
69. J.D. Whittenberger, E. Arzt, and M.J. Luton, J. Mater. Res., 5, p. 271 (1990).
70. J.D. Whittenberger, E. Arzt, and M.J. Luton, J. Mater. Res., 5, p. 2819 (1990).
71. J.D. Whittenberger, K.S. Kumar, and S.K. Mannan, Materials at High Temperature, 9, p. 3 (1991).
72. A. Kelly and K.N. Street, Proc. Roy. Soc. London, A 328, p. 283 (1972).
73. J.L. Walter and H.E. Cline, Metall. Trans., 1, p. 1221 (1970).
74. J.L. Walter and H.E. Cline, Metall. Trans., 4, p. 33 (1973).
75. D.P. Mason, D.C. Van Aken, R.D. Noebe, I.E. Locci, and K.L. King, in High Temperature Ordered Intermetallic Alloys IV, Proc. MRS, ed. by L.A. Johnson et al., 213, p. 1033 (1991).
76. R.D. Noebe, R.R. Bowman, and J.I. Eldridge, in Intermetallic Matrix Composites, Proc. MRS, ed. by D.L. Anton et al., 194, p. 323 (1990).